THREE-DIMENSIONAL MODELLINGS FOR THE VENUS-2 MOX CORE

Byung-Chan Na
OECD/NEA
Le Seine Saint-Germain, 12 Bd des Iles, 92130 Issy-les-Moulineaux, France

Nadia Messaoudi
SCK•CEN
Boeretang 200, B-2400 Mol, Belgium

Gyu-Hong Roh
Korea Atomic Energy Research Institute (KAERI)
Dukjin-dong 150, Yusong, Daejon, 305-600, Korea

ABSTRACT

Based on the VENUS-2 experimental results released by SCK•CEN, Mol, Belgium, the OECD/NEA launched a two-dimensional VENUS-2 MOX core benchmark in 1999. This was the first experiment-based benchmark and was completed in 2000. Overall, the results were very encouraging and confirmed that present methods using the latest nuclear data sets can adequately calculate MOX-fuelled systems. However, the calculation overestimated fission rates of MOX pins and slightly underestimated those of UO_2 pins. This was reflected in all combinations of computer codes and data. Therefore, a three-dimensional VENUS-2 MOX core benchmark was launched in 2001 for a more thorough investigation into the calculation methods used for MOX-fuelled systems.

This paper presents the summary of results obtained from the Monte Carlo code MCNP-4B and the deterministic code TORT calculations. Three different nuclear data sets, namely ENDF/B-VI, JENDL-3.2 and JEF-2.2 are mainly investigated. The calculated multiplication factors k_{eff} and axial pin power distributions using combinations of different data and methods are compared with the experimental results. The results obtained with different numbers of particle histories and different libraries used in MCNP-4B calculations are analysed and a comparison between the MCNP-4B and the deterministic TORT calculations is also presented. The results show that all combinations of calculation methods and nuclear data can adequately calculate the VENUS-2 MOX core in 3-D geometry, producing reasonably accurate axial pin power distributions.

1. INTRODUCTION

Use of plutonium recovered from spent fuel in the form of mixed-oxide (MOX) fuel in existing power plants is a well-established technology with many years of experience. However, since re-use of plutonium in PWRs is limited in quantity as well as in quality, the actual practice for MOX fuel use is not sufficient to stabilise the stockpile of plutonium extracted from spent fuel. For managing larger quantities through multiple recycle and high burn-up of plutonium in PWRs, it is still necessary to validate both basic nuclear data and calculation methods to understand better the behaviour of MOX fuel in challenging situations and to identify possible improvements in nuclear data and physics modelling methods.

In this context, based on the VENUS-2 experimental results released by SCK•CEN, Mol, Belgium, the OECD/NEA launched a two-dimensional VENUS-2 MOX core benchmark in 1999. This was the first experiment-based benchmark and was completed in 2000 [1]. Overall, the results were very encouraging and confirmed that present methods using the latest nuclear data sets can adequately calculate MOX-fuelled systems. However, the calculation overestimated fission rates of MOX pins and slightly underestimated those of UO_2 pins. This was reflected in all combinations of codes and data. Therefore, a three-dimensional VENUS-2 MOX core benchmark was launched in 2001 for a more thorough investigation into the calculation methods used for MOX-fuelled systems [2,3].

In the 3-D VENUS-2 measurements, the axial fission rate distributions of six fuel pins in the core were measured by γ-scanning at 21 different axial levels. The main objective of the benchmark was to calculate the axial fission rates of the 6 fuel pins and to compare them with the measured values. Additionally, fission chamber measurements (^{235}U and ^{237}Np) and activation foil measurements were performed at different axial levels at positions outside the core. These additional results could be used for a 3-D dosimetry benchmark.

This paper presents the summary of results obtained from the Monte Carlo code MCNP-4B and the deterministic code TORT calculations. Besides the ENDF60 (ENDF/B-VI based) library provided by the MCNP code package, three different nuclear data sets, namely ENDF/B-VI.5, JENDL-3.2 and JEF-2.2 are mainly investigated. The calculated multiplication factors k_{eff} and axial pin power distributions using combinations of data and methods are compared with the experimental results. A comparison of the results with different numbers of histories and different basic libraries in the MCNP-4B calculations is presented, and the differences between results from the MCNP-4B and TORT calculations are analysed.

2. BENCHMARK MODEL

The VENUS facility is a zero power critical PWR mock-up located at SCK•CEN in Belgium. As shown in Figure 1, the VENUS-2 core comprises 12 "15 × 15" subassemblies, instead of the "17 × 17" type (the pin-to-pin pitch remains typical of the "17 × 17" subassembly). The central part of the core (four 15 × 15 assemblies) consists of fuel pins 3.3 wt.% enriched in

^{235}U. There are five Pyrex pins in 1/8 of the core. Of the eight assemblies on the periphery of the core, all of which contain fuel pins 4.0 wt.% enriched in ^{235}U, eight rows of the most external fuel pins were replaced by mixed-oxide fuel pins (UO_2-PuO_2) enriched 2.0 wt.% in ^{235}U and 2.7 wt.% in high grade plutonium.

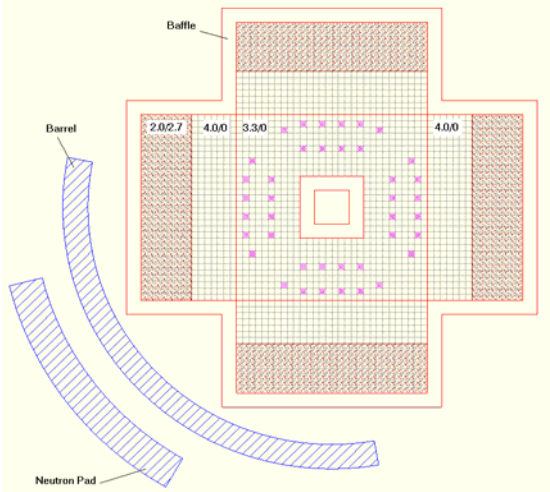

Figure 1. Horizontal cross-section of the VENUS-2 core geometry.

Figure 2 shows a vertical cross-section of the core with corresponding axial co-ordinates. The core may be divided vertically, from bottom to top, in 10 parts:

- the *reactor vessel* (stainless steel)
- the *lower filling* (water),
- the *reactor support* (water and stainless steel, not shown in the figure),
- the *bottom grid* (32.8 vol % water and 67.2 vol % stainless steel*),
- the *lower reflector* (mainly water and Plexiglas); the reflector composition changes a little from one fuel region to another, depending on the structure of the corresponding fuel pins,
- the *active height* (fuel and stainless steel),
- the *upper reflector* (mainly water and Plexiglas), including the *intermediate grid* (63.4 vol % water and 36.6 vol % Plexiglas*); the reflector composition changes a little from one fuel region to another, depending on the structure of the corresponding fuel pins,
- the *upper grid* (63.4 vol % water and 36.6 vol % stainless steel*),
- the *upper filling* (water), and
- the VENUS room environment (air).

* The given composition values assume that no pin is loaded.

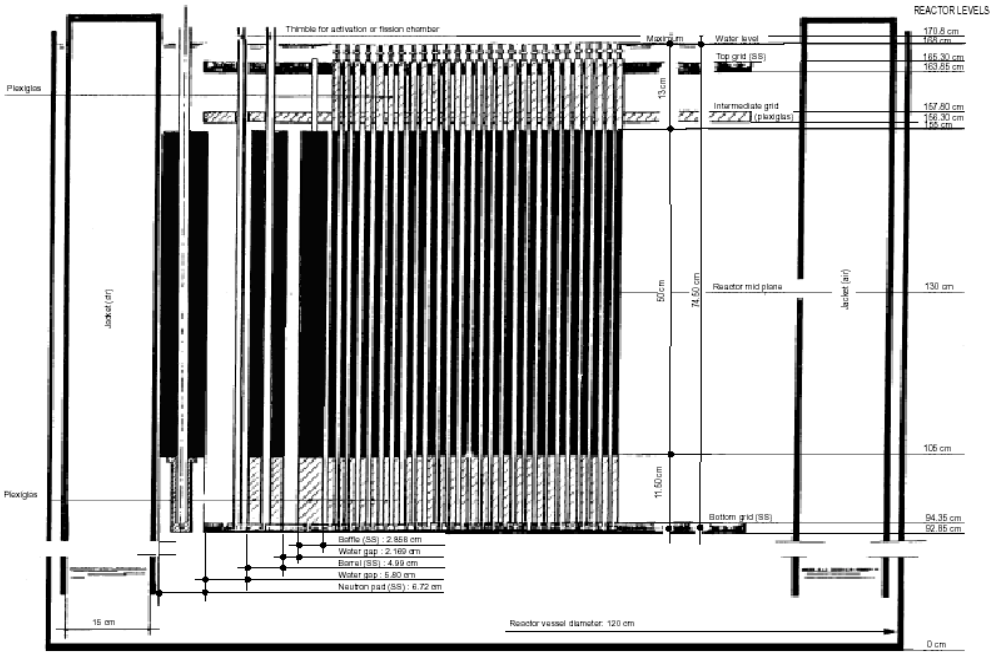

Figure 2. Vertical cross-section of the VENUS-2 reactor configuration

In the pin power measurements, one hundred and twenty-eight (128) fuel rods at the *mid-plane* of the core were measured after an irradiation of 13.5 h at 90% of the VENUS maximum power. One-eighth of the core comprises 325 fuel rods in which the pin powers of 121 fuel rods were directly measured and the pin powers of 204 fuel rods were interpolated from the measured values. The additional seven fuel pins measured were located in symmetric positions out of 1/8 of the core. The measured and interpolated positions of the fuel pins are shown in Figure 3. The pin power values were taken from the measured gamma activity of the ^{140}La and normalized to a core averaged fission rate = 1 fission/sec/fuel cell. The average fission rate in the core corresponding to absolute reference irradiation is 1.87E+08 fissions/cm/sec at the mid-plane. This average fission rate corresponds to a power of 595 watts.

In addition, the fission rate distributions of six fuel pins (*two* UO_2 3/0, *two* UO_2 4/0 and *two* MOX 2/2.7 pins) were measured **axially** by γ-scanning after an irradiation of 8 h at 90 % of the VENUS maximum power. It originally was in order to obtain vertical buckling representative of the core. These three-dimensional pin power measurement results are the subject of this benchmark.

In the VENUS-2 experiments, the co-ordinates of the measurement points can be expressed in two different co-ordinate systems: (x,y) co-ordinates *with respect to the reactor grid* and (x,y) or (r,θ) co-ordinates *with respect to the core centre*.

According to the (x,y) co-ordinates with respect to the reactor grid, the axially measured 6 pin positions are (-27, -12), (-22, -2), (-15, +2), (-13, -12), (-11, +2) and (-6, -6). These axially measured 6 pin positions are shown in Figure 3. If the (x,y) co-ordinates with respect to the

core centre are used, they are in the points (-37.17, +18.27), (-30.87, +5.67), (-22.05, +0.63), (-19.53, +18.27), (-17.01, +0.63) and (-10.71, +10.71) in cm.

The axial measurements were carried out at 21 different vertical planes along 50 cm of the fuel pin length (from 105 cm to 155 cm): starting from 110 cm, and at every 2 cm upwards to 150 cm.

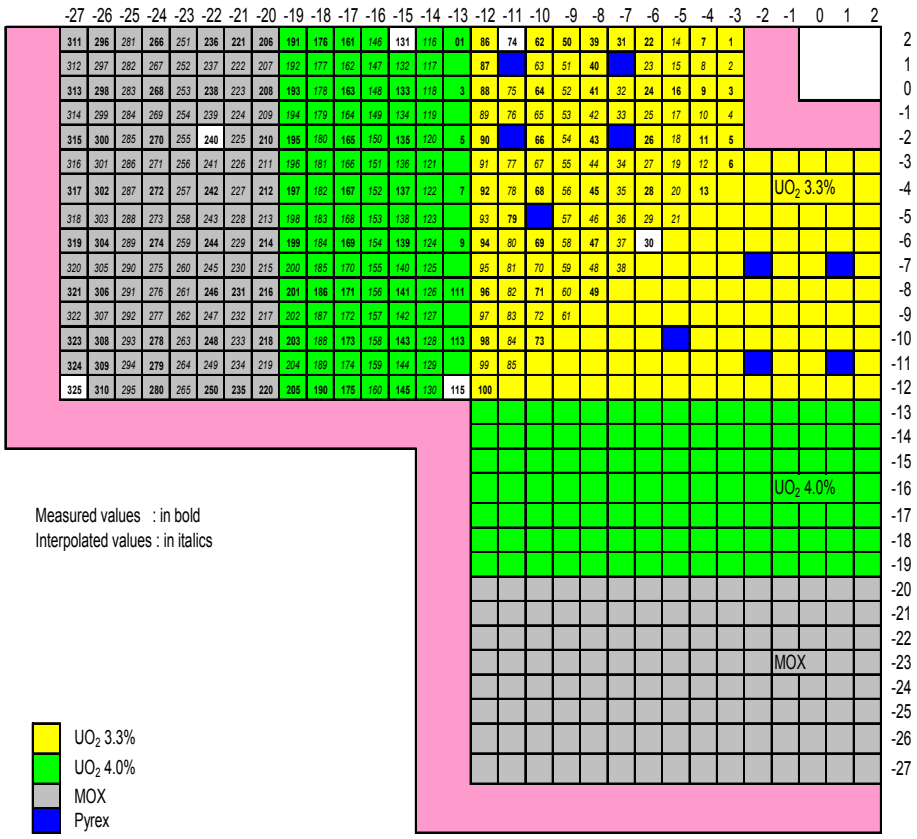

Figure 3. Measured and interpolated pin power positions in VENUS-2.

Along with all geometry and material data required to develop the detailed computational model of the 1/4 fraction of the VENUS-2 reactor core, the isotopic concentrations of each medium were provided to the participants to minimize the discrepancies of the atomic density calculations [3].

From each fuel cell calculation (UO_2 3.0, UO_2 4.0, MOX), k_∞, absorption and fission reaction rates per isotope (energy integrated and in three groups involving the 5 keV and 4 eV boundaries) were requested. From core calculations, it was requested to report k_{eff} and normalized pin power (i.e. fission rate) distribution on 1/8 of the core which consists of 325 fuel pins (normalization was to be made to a core average fission rate = 1 fission/sec/fuel cell) and normalized axial fission rates of the six fuel pins (see Figure 3). This paper will mainly discuss the calculated results of k_{eff} and of axial pin power distributions of the 6 fuel pins, compared with the experimental data.

3. CALCULATION MODELLINGS AND NUCLEAR DATA USED

Two sets of calculations were carried out using the Monte Carlo code MCNP-4B [4] and the deterministic S_N code TORT [5].

In the MCNP-4B calculations, the MCNP continuous energy neutron cross-section library ENDF60 (based on ENDF/B-VI) for all the isotopes except Sn from ENDL92, and the thermal S(α,β) library TMCCS were used as the reference, which were produced by LANL. For the purposes of comparison, three different continuous energy libraries based on ENDF/B-VI release 5, JENDL-3.2 and JEF-2.2 were newly generated by using the nuclear data processing system NJOY97.114 [6]. The fractional tolerance used in NJOY input parameter was 0.1% and the thinning option of the ACER module was not used to improve the accuracy, despite the large file size.

One quarter of the full 3-D core was explicitly modelled in three-dimensional geometry. In order to facilitate the explicit modelling of fuel rods in the core, a repeated structure option of MCNP was used. In this study, all fuel rods and Pyrex rods were fully modelled including the fuel pellet, fuel gap (*not present in MOX pin cells*), clad and coolant. The radial core components such as the reactor vessel, jacket, neutron pad, barrel, reflector, outer baffle, inner baffle and inner hole, etc. were also fully modelled. The core was modelled vertically from bottom to top, i.e., lower filling, reactor support, bottom grid, lower reflector, upper grid, upper filling, etc. In order to get the axial fission rate distributions in the core, the core was divided to 25 axial layers and the F4 tally card (track length estimate of cell flux) was used for each cell.

The number of histories originally used was 50 10^6 (100,000 neutrons/cycle and 500 cycles after 100 inactive cycles) in a reference calculation. To investigate the influence of the number of histories on calculated results, they were increased to 200 10^6 and then to 300 10^6 (100,000 neutrons/cycle and 3000 cycles after 100 inactive cycles).

A complementary set of calculations was performed using the deterministic S_N code TORT. For the cross-section generations, NJOY and TRANSX codes were used [7]. The MATXS-format 190-group neutron libraries based on ENDF/B-VI release 5 and JENDL-3.2 were generated using the MATXSR module of NJOY except for the natural Sn, which was obtained from the ENDL84 library. Using 190-group neutron libraries, ONEDANT [8] calculations for three fuel pin-cell types and a Pyrex super-cell were undertaken to obtain weight flux for generating the region-wise homogenised cross-sections collapsed to 35 groups. The TORT core calculations were carried out using the collapsed 35-group libraries.

For the preparation of the geometrical model in TORT inputs, the pre- and post-processing code BOT3P [9] was used. One quarter of the full 3-D VENUS-2 core was modelled in the (x,y,z) geometry with the S_8P_3 approximation in all TORT calculations. Fully symmetrical quadrature sets were introduced. The spatial meshes used were 100x102x72 in (x,y,z). The VENUS-2 geometry models used in the TORT calculations are shown in Figure 4. The point-wise flux convergence criterion used was 1.0E-4 and the eigenvalue convergence criterion applied was 1.0E-5.

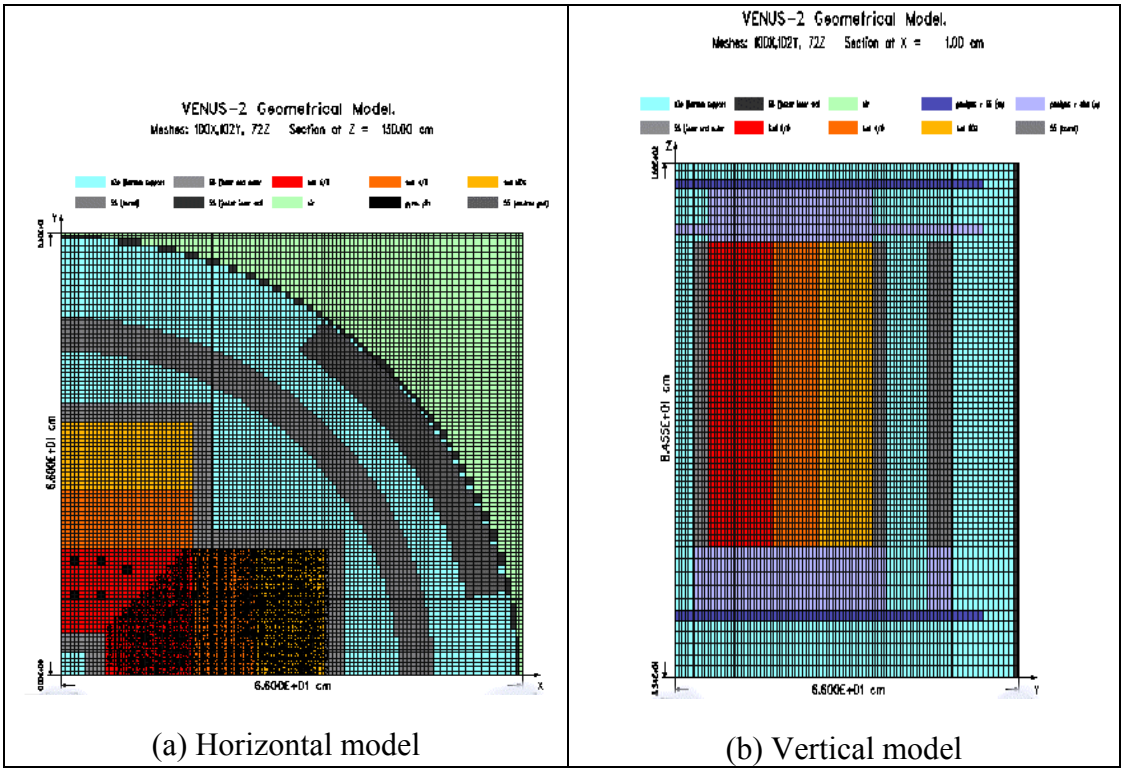

(a) Horizontal model (b) Vertical model

Figure 4. VENUS-2 geometry models in TORT calculations

No thermal scattering data for Plexiglas are available and they were not taken into account in either MCNP or TORT calculations.

4. RESULTS AND DISCUSSIONS

4.1. MULTIPLICATION FACTOR, K_{EFF}

Table 1 summarises the k_{eff} values obtained from different calculations with different libraries. The measured k_{eff} value is 1 with an uncertainty of 32 pcm.

From the MCNP-4B reference calculations (using the ENDF60 library and 50 10^6 histories), the calculated effective multiplication factor is 1.00036 ± 0.00014. Interestingly, when the number of histories is increased, even though the statistical uncertainties (1σ) decrease accordingly, the deviations from the experimental value also slightly increase to 46 pcm and 56 pcm with 200 10^6 and 300 10^6 histories, respectively. This could be remedied by increasing the number of neutrons per cycle rather than the number of cycles, and this is the subject of further investigation.

When the three libraries based on ENDF/B-VI, JENDL-3.2 and JEF-2.2 are used for the MCNP calculations with 200 10^6 histories, the deviations from the experimental value become higher: 199 pcm, 1014 pcm, 747 pcm, respectively.

Regarding the TORT solutions, the ENDF/B-VI based result gives an under-prediction of the k_{eff} value by -451 pcm, while the JENDL-3.2 based one shows an over-prediction by 511 pcm.

Table 1. k_{eff} values with different methods and libraries

Code used	Library used	Number of histories	k_{eff} (statistical uncertainty)
MCNP-4B	ENDF60	50 10^6	1.00036 (± 0.00014)
	ENDF60	200 10^6	1.00046 (± 0.00007)
	ENDF60	300 10^6	1.00056 (± 0.00006)
	ENDF/B-VI	200 10^6	1.00199 (± 0.00007)
	JENDL-3.2	200 10^6	1.01014 (± 0.00007)
	JEF-2.2	200 10^6	1.00747 (± 0.00007)
TORT	ENDF/B-VI	-	0.99549
	JENDL-3.2	-	1.00511

4.2. AXIAL PIN POWER (FISSION RATE) DISTRIBUTIONS

Before analysing the axial pin power results, it should be noted that the reported uncertainties of the measured data (1σ) of the six fuel pins are ±2.2% in UO_2 and ±3.4% in MOX pins.

Results of MCNP reference calculation

A MCNP reference calculation with the ENDF60 library was performed for 50 10^6 histories (100,000 neutrons/cycle and 500 cycles). The results of this reference calculation are shown in Figures 5 to 7 for the MOX, UO_2 4/0, and UO_2 3/0 pins, respectively. The x-axis represents the axial positions of measured pins and the y-axis represents the discrepancy between calculated and measured pin power values.

The scatter bands are about ±4% for the MOX pins and about ±2% for the UO_2 pins, except for a few axial pin positions. The standard deviations of differences between calculated and measured values are 3.5% for the MOX pin (-27,-12) and 2.9% for the MOX pin (-22,-2). For the UO_2 4/0 pins, the calculated pin power distributions show an excellent agreement compared with the experimental values. For most of the axial positions, the scatter band is within ±2%. The standard deviations of differences between calculated and measured values are 1.8% for the UO_2 pin (-15,+2) and 1.5% for the UO_2 pin (-13,-12). For the UO_2 3/0 pins, even though the agreement is good for most of the axial positions, the scatter band becomes larger especially near the upper part of the core. As a result, the standard deviations of

differences between calculated and measured values are 2.5% for the UO_2 pin (-11,+2) and 2.3% for the UO_2 pin (-6,-6). This may be due to ignoring the thermal scattering by Plexiglas which is the main composition of the axial reflectors.

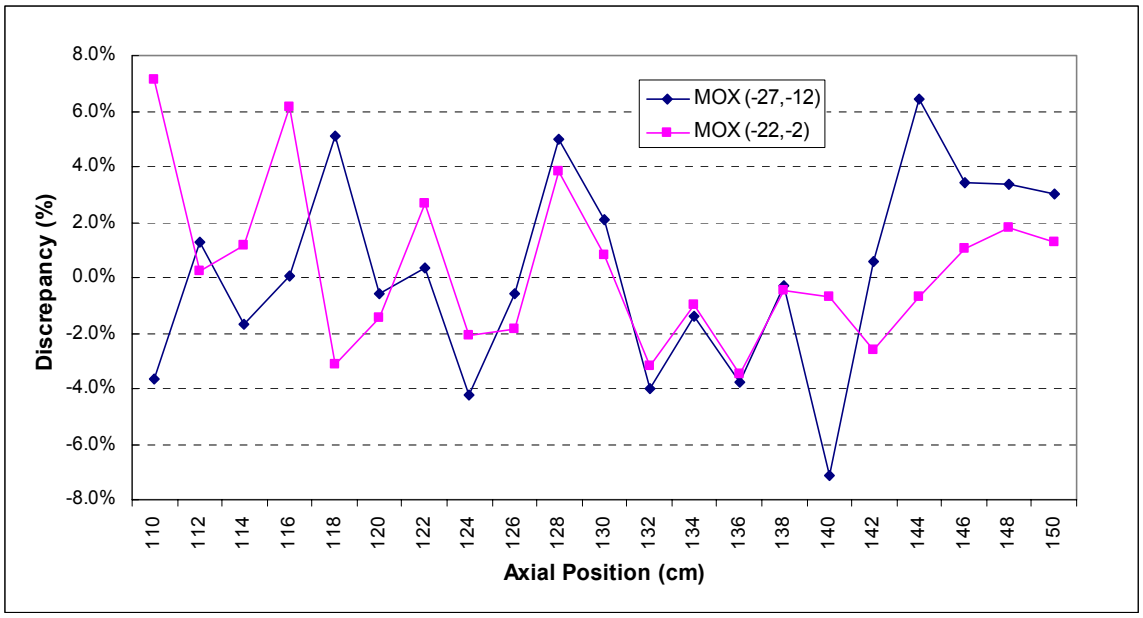

Figure 5. MCNP reference calculation results for the MOX pins

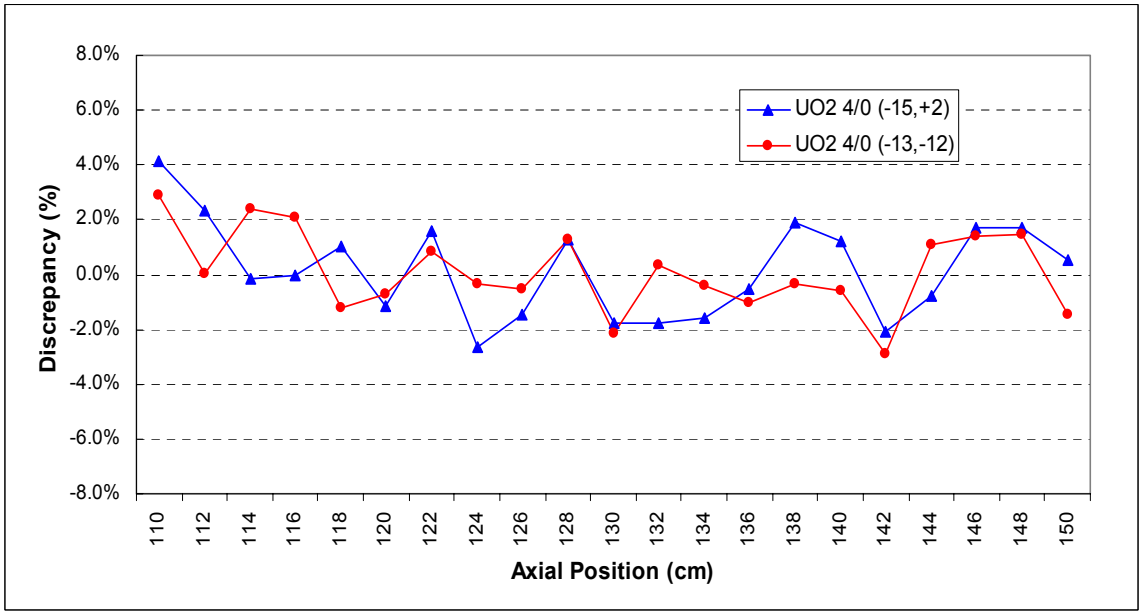

Figure 6. MCNP reference calculation results for the UO_2 4/0 pins

The relative errors (1σ) are about 3% for the MOX pin (-27,-12) and about 2% for the MOX pin (-22,-2), while they are about 1.5% for the four UO_2 pins. The relative errors are always slightly higher at positions near the axial reflectors, which may explain a worse agreement of the calculated axial power distributions in the UO_2 3/0 pins near the upper reflector.

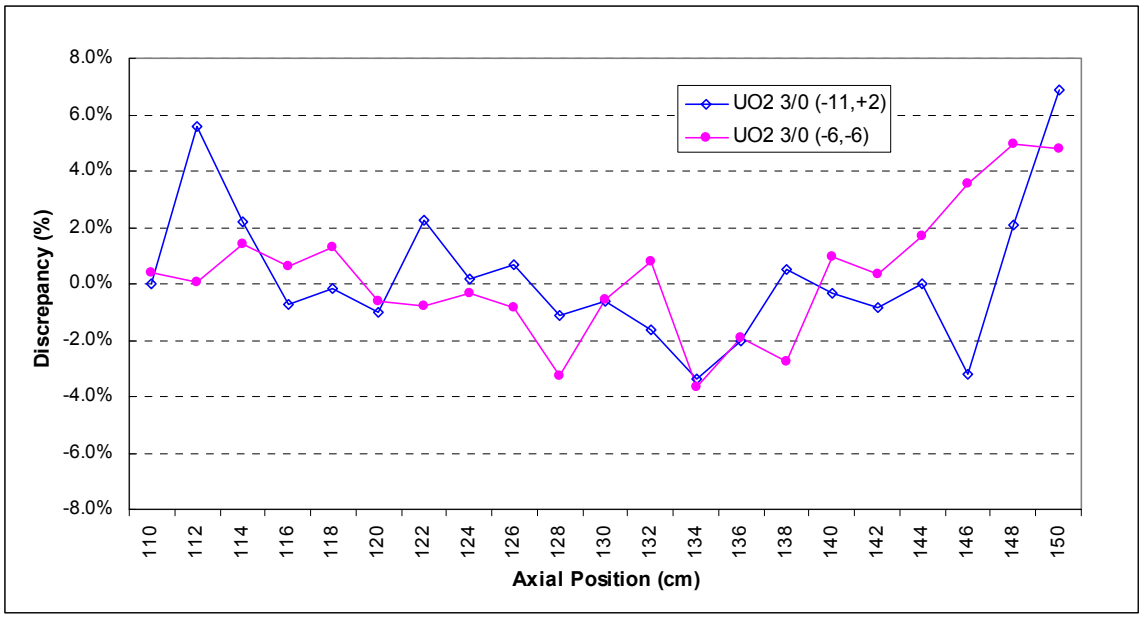

Figure 7. MCNP reference calculation results for the UO_2 3/0 pins

If the relative errors can be further decreased, a better scatter band could be obtained especially for the MOX pins and a worse agreement of the calculated axial power distributions in the UO_2 pins near the axial reflectors (so-called reflector effect) would be remedied to some extent.

Influence of number of particle histories on MCNP calculation results

For the following comparison, all the calculations were carried out with the ENDF60 library, increasing the number of histories for each step. The comparative results for the MOX pin (-27,-2) and for the UO_2 3/0 pin (-11,+2) are presented in Figures 8 and 9.

When the number of histories is increased to 200 10^6, the relative errors (1σ) are about 1.7% for the MOX pin (-27,-12) and about 0.9% for the MOX pin (-22,-2), while they are about 0.7% for the four UO_2 pins. In consequence, the scatter bands become much smaller for both MOX and UO_2 pins than in the reference calculation with 50 10^6 of histories. However, the reflector effect still exists especially for the UO_2 pins. For the MOX pins, out of the 21 axial measured positions, 20 positions give less than 3% of discrepancy, which is less than the reported uncertainty of the measurement (±3.4%). In the UO_2 pins, for most of the axial positions (more than 18 positions for the UO_2 4/0 and 15 for UO_2 3/0 pins), the agreements between calculated and measured pin power values are very good (less than ±2%). The slightly worse results for the UO_2 pins are due to the pronounced reflector effect near the

axial upper and lower reflectors. This means that an increase in the number of histories cannot totally remedy the reflector effect.

The standard deviations of differences between calculated and measured values are 1.7% for the MOX pin (-27,-12) and 2.0% for the MOX pin (-22,-2). For the UO_2 4/0 pins, the standard deviations of differences between calculated and measured values are 1.1% for the UO_2 pin (-15,+2) and 1.4% for the UO_2 pin (-13,-12). For the UO_2 3/0 pins, the standard deviations of differences between calculated and measured values are 1.8% for the UO_2 pin (-11,+2) and 1.8% for the UO_2 pin (-6,-6).

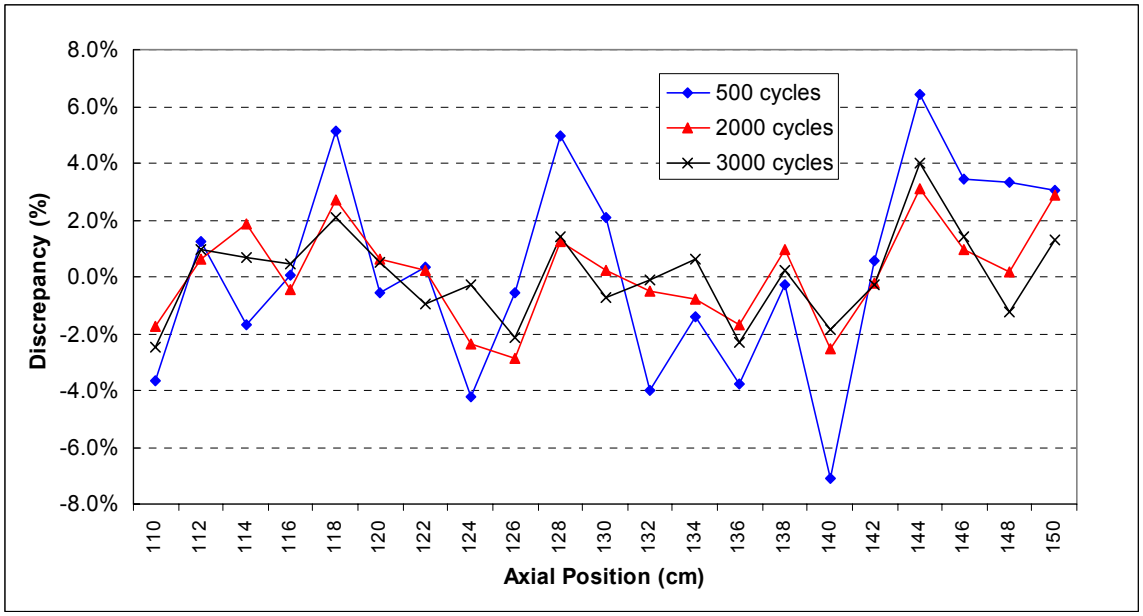

Figure 8. MCNP results with different histories for the MOX pin (-27, -12)

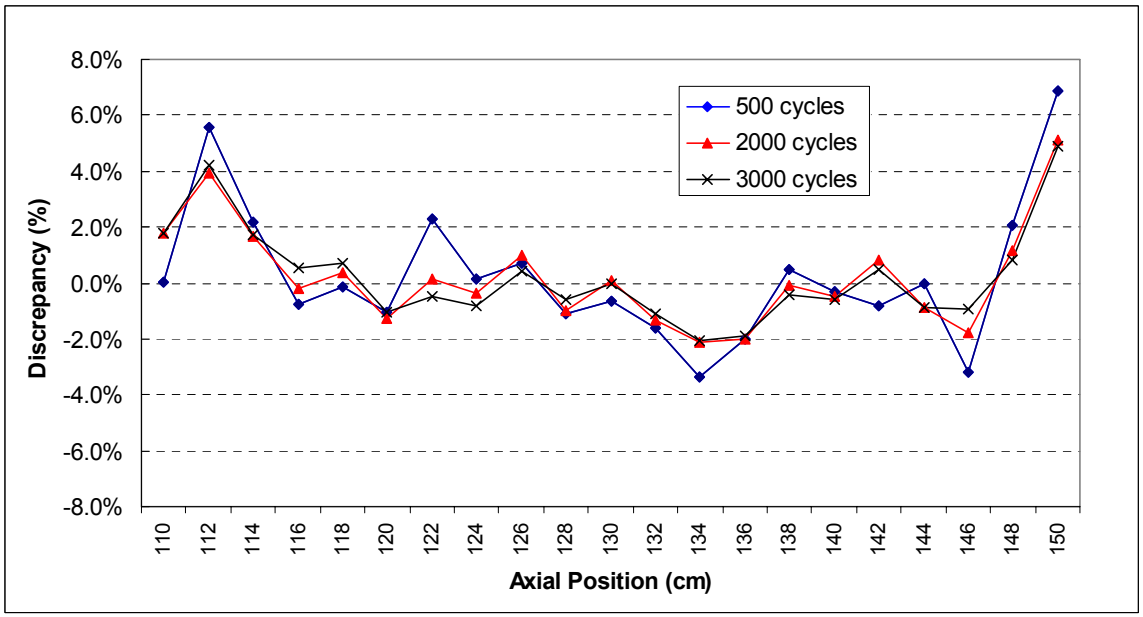

Figure 9. MCNP results with different histories for the UO_2 3/0 pin (-11, +2)

To examine more thoroughly the influence of the number of histories on results, the histories were again increased up to 300 10^6. From the latter calculation, the reported relative errors (1σ) are about 1.3% for the MOX pin (-27,-12) and about 0.6% for the MOX pin (-22,-2), and they are about 0.7% for the four UO_2 pins. However, the pin power results obtained show almost the same trend as those from the calculations with 200 10^6 cycles. The standard deviations of differences between calculated and measured values are 1.6% for the MOX pin (-27,-12) and 1.9% for the MOX pin (-22,-2). For the UO_2 4/0 pins, the standard deviations of differences between calculated and measured values are 1.1% for the UO_2 pin (-15,+2) and 1.5% for the UO_2 pin (-13,-12). For the UO_2 3/0 pins, the standard deviations of differences between calculated and measured values are 1.8% for the UO_2 pin (-11,+2) and 1.8% for the UO_2 pin (-6,-6).

Therefore, compared to the calculation results with 200 10^6 histories, no real gain is obtained when the number of histories is increased up to 300 10^6. As observed in the calculated k_{eff} results, an increase in the number of neutrons per cycle rather than that in the number of cycles would give better results of power distributions. This point will be further investigated in the following study.

Influence of the different libraries on MCNP calculation results

For the comparison of results with different libraries, the ENDF60-based MCNP calculations with 200 10^6 histories were taken as the reference case and the MCNP calculations with the three different libraries were undertaken for the same number of histories. The results for the MOX pin (-22,-2) and the UO_2 4/0 pin (-13,-12) are shown in Figures 10 and 11.

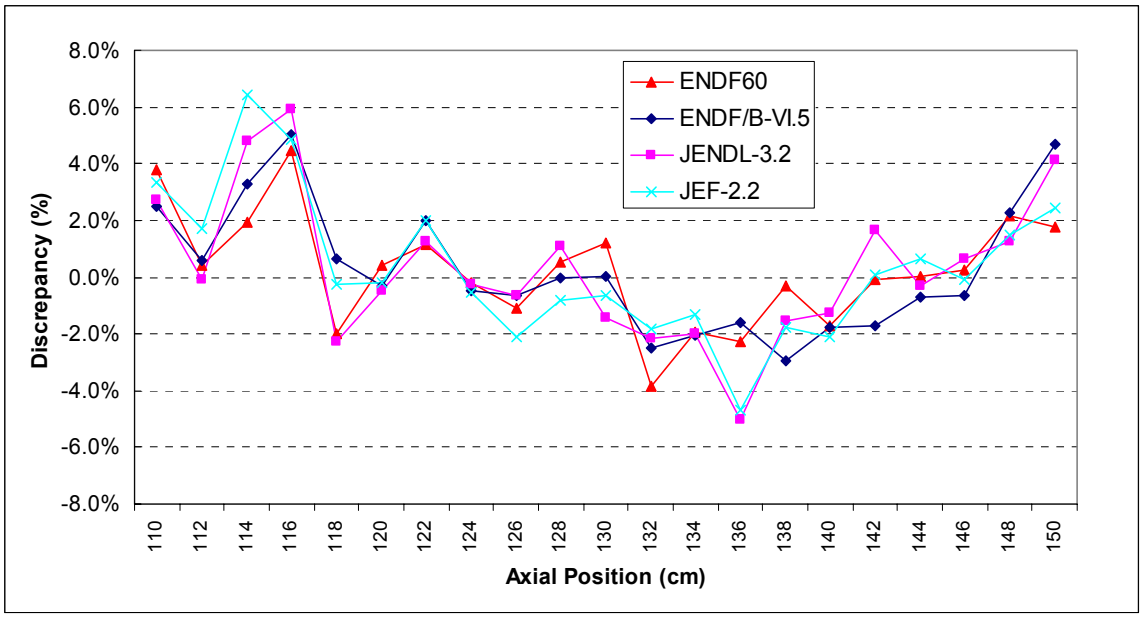

Figure 10. MCNP results with different libraries for the MOX pin (-22, -2)

A general observation on the results of all four calculations is that for most of the axial pin positions the calculated pin power results show the discrepancies within ±2% compared to the experimental values.

For the MOX pin (-27,-12), the JENDL-based results give slightly better results than those based on ENDF60. The worst results are those based on JEF. For the MOX pin (-22,-2), the three different libraries give almost the same results. Among them, the ENDF/B-VI results are slightly better than the others. The best solutions are given by the ENDF60-based calculations.

For the four UO_2 pins, all calculations with the four different libraries give almost the same results. The agreements between calculated and measured pin powers for the UO_2 pins are better than those for the MOX pins in all results. The reflector effect is also shown in all calculations, especially for the UO_2 pins.

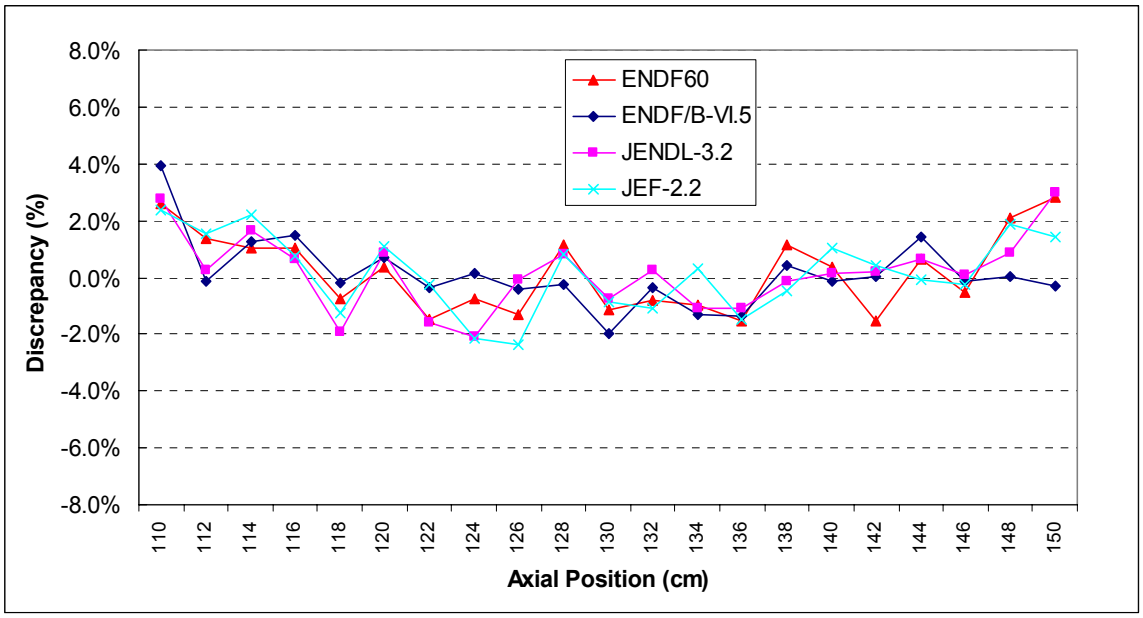

Figure 11. MCNP results with different libraries for the UO_2 4/0 pin (-13, -12)

Comparison of MCNP and TORT results

Two sets of the TORT calculations were performed using the libraries based on ENDF/B-VI and JENDL-3.2. In two TORT calculations, the same geometry models and angular approximations were used. The TORT results were compared to the MCNP results with 200 10^6 histories which applied the same libraries. The results for the MOX pin (-27,-12) are presented in Figure 12.

Surprisingly, the differences between the two different libraries are very small in the TORT calculations, contrary to those in the MCNP calculations. Even though it is not possible to give a clear explanation on this, it may be explained by the fact that the TORT calculations do not suffer from the statistical perturbation as the MCNP calculations. In other studies,

when different spatial mesh sizes are used in deterministic calculations, the calculation results are different even when using the same library. The mesh size effect in the TORT calculations will be further investigated.

For the two MOX pins, the TORT calculations give slightly better results than the MCNP calculations when the ENDF/B-VI library is used. The two JENDL-based results show almost the same scatter bands in both calculations. For the UO_2 pins, the TORT calculations give almost the same results as the MCNP calculations and the reflector effect is also shown in the TORT results.

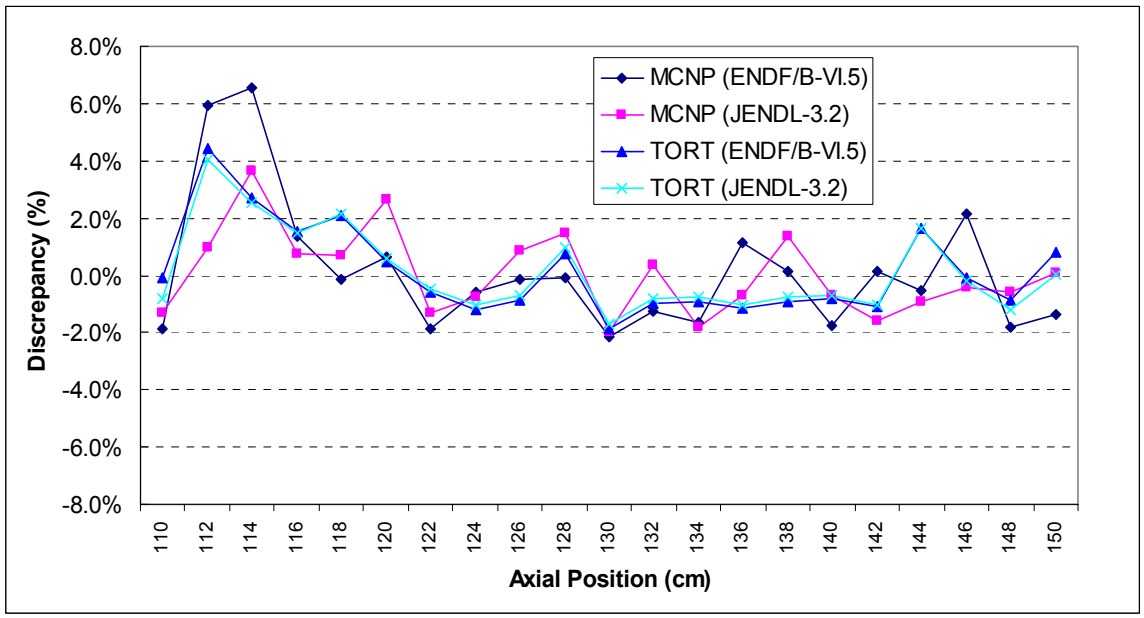

Figure 12. MCNP and TORT results for the MOX pin (-27, -12)

5. CONCLUSIONS

An international benchmark exercise based on the three-dimensional VENUS-2 MOX core experiment results was organised in the framework of OECD/NEA. The benchmark aimed at validating three-dimensional calculation methods together with the latest nuclear data used for MOX-fuelled systems. Therefore, the measured axial pin power distributions of the 6 fuel pins at 21 axial positions were mainly investigated in the benchmark.

Two sets of calculations were performed involving both deterministic and Monte Carlo reactor analysis methods using three different nuclear data sets, namely ENDF/B-VI.5, JENDL-3.2, and JEF-2.2. The ENDF60 (ENDF/B-VI based) library provided by the MCNP code package was also applied. The codes used in this study are the Monte Carlo code MCNP-4B and the deterministic S_N code TORT. One quarter of the full 3-D core was modelled in three-dimensional geometry in both types of calculations.

Regarding the calculated k_{eff} values, the TORT results based on ENDF/B-VI.5 and JENDL-3.2 show a discrepancy by 0.5% compared to the experimental value. As for the MCNP results, the ENDF60-based values are in excellent agreement with the experimental value (less than 0.05% of discrepancy), while ENDF/B-VI.5 and JEF-2.2 give values with a discrepancy of 0.2% and of 0.75%, respectively. The JENDL-3.2 based MCNP result gives surprisingly a higher value by about 1.0% of discrepancy. The difference between the JENDL-based TORT and MCNP calculations is about 500 pcm.

As for the axial pin power distributions, a MCNP reference calculation with the ENDF60 library and 50 10^6 histories (100,000 neutrons/cycle and 500 cycles) gives a scatter band of about ±4% for the MOX pins and about ±2% for the UO_2 pins, except for a few axial pin positions. These results are reasonably good, taking into account the reported uncertainties of the measured data (1σ) which are ±2.2% in UO_2 and ±3.4% in MOX pins. However, the scatter band becomes larger near the axial upper and lower reflectors of the core, especially for the UO_2 3/0 pins, even though the agreement is good for most of the axial positions. This may be due to ignoring the thermal scattering by Plexiglas which is the main composition of the axial reflectors.

When the number of histories is increased to 200 10^6, the scatter bands become much smaller for both MOX and UO_2 pins than in the reference calculation with 50 10^6 histories. For the MOX pins, out of the 21 axial measured positions, 20 positions give less than 3% of discrepancy, which is less than the reported uncertainty of the measurement (±3.4%). In the UO_2 pins, for most of the axial positions (more than 18 positions for the UO_2 4/0 and 15 for UO_2 3/0 pins), the agreements between calculated and measured pin power values are very good (less than ±2%). However, the reflector effect still exists for the UO_2 pins. No real gain is obtained when the number of histories is increased to 300 10^6.

From an intercomparison of the MCNP results based on the four different libraries (ENDF60, ENDF/B-VI.5, JENDL-3.2 and JEF-2.2), a general observation is that there are no big differences in the four calculation results and that, for most of the axial pin positions, the calculated pin power results show the discrepancies within ±2% compared to the experimental values. Therefore, it cannot be said which library is the best.

The TORT calculations produce very similar results to the MCNP calculations for both MOX and UO_2 pins. The differences between the two libraries (ENDF/B-VI and JENDL-3.2) are very small in the TORT calculation results, contrary to those in the MCNP calculations. This may be due to the fact that the TORT calculations do not suffer from the statistical perturbation as the MCNP calculations. The reflector effect is also shown in the TORT results for the UO_2 pins.

In general, all combinations of calculation methods and nuclear data can adequately calculate the VENUS-2 MOX core in 3-D geometry, producing reasonably accurate axial pin power distributions.

As a follow-up, the origin of reflector effect observed for UO_2 pins in both MCNP and TORT calculation results will be further investigated, taking into account thermal scattering of

Plexiglas (or that of a similar material). The influence of different spatial and angular approximations on axial pin power results will also be studied in TORT calculations.

REFERENCES

1. Byung-Chan Na, "Benchmark on the VENUS-2 MOX Core Measurements," OECD/NEA report, NEA/NSC/DOC(2000)7, ISBN 92-64-18276-4, December 2000.

2. K. van der Meer, et al., "Additional Data for the 3-D VENUS-2 Benchmark," SCK•CEN report, TN-0008, September 2000.

3. Byung-Chan Na and Nadia Messaoudi, "Blind Benchmark on the 3-D VENUS-2 MOX Core Benchmark," Final Specification, NEA/SEN/NSC/WPPR(2001)1, May 2001.

4. J. F Briesmeister, ed., "MCNP – A General Monte Carlo N-Particle Transport Code, Version 4B," LA-12625-M, Los Alamos National Laboratory, 1997.

5. "TORT-DORT: Two- and Three-Dimensional Discrete Ordinates Transport, Version 2.7.3," RISCC code package CCC-543, Oak Ridge National Laboratory, May 1993.

6. R.E. MacFarlane and D.W. Muir, "The NJOY Data Processing System Version 91," LA-12740-M, Los Alamos National Laboratory, 1994.

7. "TRANSX 2.15: Code System to Produce Neutron, Photon, and Particle Transport Tables for Discrete Ordinates and Diffusion Codes from Cross Sections in MATXS Format," PSR-317, Los Alamos National Laboratory, February 1995.

8. R.E. Alcouffe, et al., "DANTSYS, A Diffusion Accelerated Neutral Particle Transport Code System," LA-12969-M, Los Alamos National Laboratory, 1995.

9. R. Orsi, "The ENEA-Bologna Pre-Post Processor Package BOT3P for the DORT and TORT Transport Codes (Version 1.0)", December 1999.